Journal of Hydrology 569 (2019) 373–386

Contents lists available at ScienceDirect

Journal of Hydrology

journal homepage: www.elsevier.com/locate/jhydrol

Research papers

Characterizing the Indian Ocean sea level changes and potential coastal flooding impacts under global warming

K.S. Carvalho, S. Wang*

Department of Land Surveying and Geo-Informatics, Hong Kong Polytechnic University, Hong Kong, China

ARTICLE INFO

This manuscript was handled by Geoff Syme, Editor-in-Chief

Keywords:
Flooding
Indian Ocean
Interpolation
Inundation mapping
Sea level

ABSTRACT

The Indian Ocean which is home to many islands and the low-lying coastal zones have attracted considerable attention due to regional sea level changes. In this study, we examine regional changes in sea level of the Indian Ocean and potential coastal flooding impacts by using tide gauge data. Various interpolation methods are evaluated to predict values at locations where data is unavailable. Based on the cross-validation analysis, the radial basis function is identified as the most optimal interpolation method and is used to analyze the spatial patterns of sea level changes. The analysis reveals that Bangladesh, Seychelles, and Cocos (Keeling) Islands have relatively high rates of sea level rise. These regions would thus be highly vulnerable to coastal flooding induced by the accelerating sea level rise in future decades, posing significant threats to coastal communities and ecosystems. Flooding impacts are examined through inundation mapping in a geographic information system (GIS) environment. In addition, relationships between regional factors (sea surface temperature, air temperature, and vertical land motions) affecting sea level rise are investigated. Our findings indicate that vertical land motion is an important factor affecting sea level changes for the regions of Seychelles and Cocos Islands. There is a strong relationship between air temperature and sea level rise for all studied regions. This study is a first attempt to examine regional changes in sea level of the Indian Ocean and potential coastal flooding impacts by using tide gauge data. The methods used in this study can be applied to other coastal regions around the world.

1. Introduction

Historical sea level records from warm periods during the last 3 million years indicate that the global mean sea level has exceeded 5 m above the present day scenario. Recent trends of thinning of glaciers such as Greenland and Antarctic Ice Sheets have raised a growing concern (Gornitz, 2013). The contribution made by these two ice sheets has greatly increased since the 1990s due to increased outflow caused warming of immediate adjacent oceans. Global sea level has risen during the past few decades as a consequence of the thermal expansion of warming oceans and the addition of freshwater from melting continental ice sheets (Han et al., 2010). Thermal expansion is one of the dominant factors in sea level rise and is a consequence of sea surface temperature (Pramanik et al., 2015).

Sea level changes are not uniform globally (Church et al., 2004; Hay et al., 2015; Merrifield et al., 2016). Regional sea level changes can be affected by oceanic and atmospheric circulation and other factors that can alter sea surface heights. In addition, there are a variety of factors that can cause vertical land movements such as sediment compaction, the compaction caused by groundwater extraction and other geological processes related to plate tectonics and Earth movements. Localized vertical land motions (VLM) have a significant impact on regional sea level changes (Wöppelmann and Marcos, 2016). The downward VLM (land subsidence) and the upward VLM (land uplift) can cause a rise or fall in sea levels (Sweet et al., 2017).

The Indian Ocean has been warming faster than other oceans (Roxy et al., 2014). And the in-situ hydrographic records have proven that the Pacific Ocean is likely responsible for the decrease in the ocean heat content of the Pacific over the past few decades. The heat originally stored in the Pacific is being transported to the Indian Ocean by the Indonesian throughflow. Han et al. (2010) revealed that anthropogenic warming effects on the Indo-Pacific ocean pool can result in sea level variations and changes in atmospheric circulation by using ocean circulation modes (The Hybrid Coordinate Ocean Model and the Parallel Ocean Program). The entire Indian Ocean has been undergoing warming for the past century. From 1901 to 2002, the western sea surface temperature has been increasing at a greater rate as compared to other parts of the Indian Ocean (Roxy et al., 2014). According to the National Centre for Antarctic and Ocean Research, the sea levels in the Indian Ocean are almost double than the global mean. Due to the

* Corresponding author.
E-mail address: shuo.s.wang@polyu.edu.hk (S. Wang).

https://doi.org/10.1016/j.jhydrol.2018.11.072
Received 23 October 2018; Received in revised form 28 November 2018; Accepted 30 November 2018
Available online 20 December 2018

location of the Indian Ocean, wind and heat play a dominant role in this region whereas melting of ice caps and glaciers are a negligible occurrence.

Sea level rise threatens the densely populated and low-lying coastal areas (Khan et al., 2000; Qin and Lu, 2014). It has already caused floods and devastating storms that have impacted many lives over recent years. Regional sea level rise can vary from place to place depending on many factors such as ocean winds, temperatures, and land motions. An acceleration in sea level rise has been detected in the northern parts of the Indian Ocean. Due to changing wind speeds and distribution of heat, certain parts of the Indian Ocean north of the equator have experienced an increase in sea level rise (Thompson et al., 2016). As an evolving issue in a changing climate, it is necessary to assess the impacts of sea level rise and to highlight those regions of the world which are highly prone to its consequences.

The performance of tide gauges has been attracting considerable attention over the past few decades. With great improvements in data quality and high-frequency data, tide gauges have replaced the traditional float gauges and have been widely used in sea level rise studies (Míguez et al., 2012). For example, Baki and Shum (2000) used tide gauge observations from the Hong Kong Observatory to investigate sea level variations in Hong Kong. Han et al. (2010) combined tide gauge and satellite observations of Indian Ocean sea level with climate-model simulations to identify a distinct spatial pattern of sea-level rise since the 1960s. Pramanik et al. (2015) used tide gauge data to map sea level changes along the East Coast of India and determined the coastal vulnerability. However, previous studies have not looked into the regional factors that affect local sea level changes. Moreover, there is a lack of assessing potential coastal flooding threats caused by sea level rise in the Indian Ocean. It is thus necessary to produce inundation maps that can be used to help identify flood-prone areas, which plays a crucial role in protecting coastal communities from rising sea levels.

Tide gauge data collected from stations can help better understand the current trends in sea level changes. However, tide gauge stations are unevenly distributed around the globe, thereby resulting in large gaps and difficulties in performing spatial analysis. As a result, spatial interpolation techniques are essential for creating a continuous surface from sampled point values (Wang et al., 2014, 2015). In the past, a variety of interpolation methods were used to map climate variables. For example, Agnew and Palutikof (2000) used the ordinary Kriging which was a GIS-based geostatistical interpolation approach for creating high-resolution maps of mean seasonal temperatures and precipitation in the Mediterranean Basin. Keskin et al. (2015) mapped precipitation, wind speed, and temperature over Turkey in a GIS environment. The GIS-based interpolation techniques have been recognized as a powerful means to create continuous surfaces from point data. Since spatial interpolation methods are data-specific or variable-specific, there is no best choice among the interpolation methods available. The best option of interpolation methods in a particular case can thus be obtained by comparing their performance. Few studies have compared the performance of the GIS-based interpolation techniques for producing spatial patterns of sea level changes from tide gauge observations.

The objective of this study is to examine the Indian Ocean sea level changes over the last 80 years and potential coastal flooding impacts by using tide gauge data. A comparison of spatial interpolation methods will be conducted to generate spatial patterns of sea level changes in the Indian Ocean. Coastal flooding impact areas will then be delineated through the inundation mapping for countries that have relatively high rates of sea level rise. Relationships between regional factors and sea level rise as well as their contributions to sea level changes will also be investigated through multivariate regression analysis.

This paper is organized as follows. Section 1 provides an overview of sea level rise, limitations of previous studies, and objectives of this study. Section 2 introduces the study area, sources of datasets, GIS-based interpolation methods used to create continuous surfaces of sea level changes, flood inundation mapping, and regression models. Section 3 presents a thorough analysis and discussion on comparisons of interpolation methods, relationships between regional variables and sea level changes, and potential impacts of sea level rise on coastal flooding. Finally, conclusions drawn from this study are summarized in Section 4.

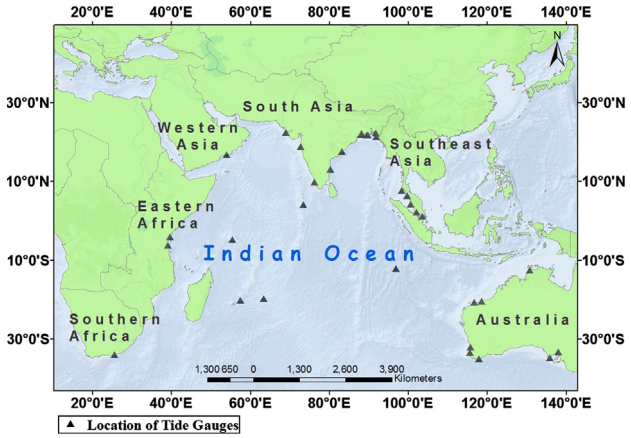

Fig. 1. Indian Ocean with locations of tide gauge stations.

2. Case study, data, and methodology

2.1. Study area

The Indian Ocean is the world's third largest ocean with a total area of 70,560,000 km^2, which lies between latitudes 30°N to 35°S and longitudes 20°E to 140°E. The Indian Ocean is surrounded by African, Asian and Australian continents, which is home to many low-lying coastal regions and islands (Li and Han, 2015). These low-lying areas are vulnerable to sea level rise and coastal flooding (Church et al., 2006). Fig. 1 shows the study area with the locations of tide gauge stations.

One of the most damaging impacts of climate change is sea level rise. Since 160 million people currently live in coastal regions that are less than 1 m above sea level, a small magnitude of rise in sea levels can pose significant threats to human population and damage infrastructure near the coastlines. In this study, spatial patterns of sea level changes were analyzed and potential coastal flooding impacts were then examined by using inundation maps for the countries that had relatively high rates of sea level rise.

2.2. Data collection

Tide gauge data has not been used to assess sea level changes in the Indian Ocean, which brings more attention to this study. Unlike satellites that were launched in the mid-1990s, the use of tide gauges provided an idea of long-term historical changes in sea level. Coastal ocean tide gauge time series contain unique information about historical basin-scale variability as well as information about global sea level rise (Chepurin and Carton, 2013). Used in harbor operations, the tide gauge data facilitates studying phenomena in the supra-hourly range with useful applications in storm surge and tsunami monitoring (Míguez et al., 2012). Thus, this study used historical data provided by tide gauges in assessing the changes in sea level in the Indian Ocean. Due to their sparse distribution along the countries, data were chosen based on two factors including data availability (i.e. long-term time series) and minimal gaps in data collected. In this study, a thorough investigation on all tide gauge stations was conducted in the first place to decide which stations had updated readings. The tide gauge data over a long time period of up to 60 years were then collected. Since tide

gauge stations may have missing data for certain years, the stations with small data gaps (less than 3 years) were chosen to perform time series analysis.

Tide gauge records from the data archive of the Permanent Service for Mean Sea Level (PSMSL) Revised Local Reference (RLR) were used in this study. The PSMSL contains monthly and annual mean values of more than 2000 tide gauge stations distributed around the world. The data is received by national authorities who are responsible for monitoring sea level changes for particular countries or regions. Constructing time series of the sea level measurements at each station requires monthly and annual means be reduced to a common datum. This reduction was performed by making use of the tide gauge datum history provided by the supplying authorities. The RLR datum at each station is defined to be approximately 7000 mm below mean sea level, and an arbitrary choice is made so as to avoid negative values in the datasets. Since the primary focus is on sea level time series analysis, no glacial isostatic adjustment (GIA) corrections have been performed.

Sea surface temperature (SST) was obtained from the National Oceanic and Atmospheric Administration (NOAA) Optimal Interpolation (OI) SST dataset provided by the NOAA Earth System Research Laboratory's Physical Sciences Division (https://www.esrl.noaa.gov/psd/). The NOAA OI SST dataset was constructed by combining observations from different platforms including satellites, ships, and buoys. Air temperature is another factor considered in this study, we analyzed the relationship between air temperature and sea level rise. The air temperature data was acquired from the Climate Change Knowledge Portal website as part of the World Bank Group. This website provides a wide range of information on climate change around the world. This portal was designed to help policy makers and practitioners in using scientific information to make informed decisions and provide valuable information to the end users for projects and research.

Along any coast, VLM of the sea or the land can cause variations in sea level relative to land. Coastal subsidence and uplift can aggravate the problem of sea level rise, and measuring VLM is a fundamental key in coastal flood risk management and estimating the needs of the ecosystems worldwide. To measure VLM on the Earth, GPS stations, satellite altimetry, and tide gages spanning the entire globe located between 66°N and 66°S can provide easily accessible data for climatological studies. Tide gauges measure sea level relative to the Earth's crust and thus the measurements are affected by VLM. Satellite altimetry measurements are generally independent; the sea level measured is with respect to the geocenter and is thus independent of VLM. VLM is contained in the long-term component of the difference between satellite altimetry and tide gauge sea level height measurements and is indicated as "Altimetry – Tide Gauge" or "ALT-TG" (Fenoglio et al., 2012).

In this study, altimetry data were used to explore VLM in the areas with the highest rates of sea level rise. The satellite altimetry data is defined as the Global MSLA heights in delayed time ("all sat merged") and is provided by AVISO. Further information about the Altimetry measurements can be obtained from SONEL (www.sonel.org) data service.

2.3. Spatial interpolation methods

In this study, we compared all GIS-based interpolation methods for creating sea level change surfaces over the Indian Ocean, including inverse distance weighting (IDW), local polynomial interpolation (LPI), global polynomial interpolation (GPI), radial basis function (RBF), ordinary Kriging (OK) and universal Kriging (UK). They can be divided into two groups, including deterministic and geostatistical techniques. The deterministic interpolation methods (i.e. IDW, LPI, GPI and RBF) create continuous surfaces from measured points based on mathematical formulae to determine the extent of similarity or degree of smoothing, while the geostatistical interpolation methods (i.e. OK and UK) use both mathematical and statistical models to predict the values within the given area of interest and provide probabilistic estimates of the interpolation quality based on the spatial autocorrelation among the points. The OK method depends on the strong assumption of stationarity (the mean and variance of the values are constant across the spatial field) which is not often met in many applications. In comparison, the UK method relaxes the assumption of stationarity by allowing the mean of the values to vary across the spatial field. Details for each of these interpolation methods are provided as follows.

2.3.1. IDW method

The IDW method is used when the density of sampled points is high enough to capture the extent of the surface variations needed for spatial analysis. It is based on the principle that the sampled values closer to the prediction location have a greater influence on the prediction value as compared to sampled values which are further apart. A higher power assigns more weight to closer points, resulting in less smoother surfaces. Contrarily, a lower power assigns a low weight to closer points, resulting in a smoother surface. The IDW specifically relies on the First Law of Geography. The formula for the IDW is given below:

$$Z = \frac{\sum_{i=1}^{n} \frac{1}{(d_i)^p} Z_i}{\sum_{i=1}^{n} \frac{1}{(d_i)^p}} \quad (1)$$

where Z is the predicted value of the interpolation point; Z_i is the value of the sampling point i (i = 1, 2, 3 …n); n is the number of sample points; d_i is the distance between known and unknown sample points; p is the power parameter which is a real positive number.

2.3.2. GPI method

The GPI uses a mathematical function (a polynomial) to fit a smooth surface over sample points. In contrast to the IDW, the GPI makes predictions using the entire dataset instead of using the measured points within neighborhoods. A first-order global polynomial can fit a single plane through given data. And a second-order polynomial creates a bended surface. It should be noted that complex polynomials may result in difficulties in representing physical meanings. In addition, a single global polynomial may not be able to fit a surface with varying shape (e.g., slope variations), and thus multiple polynomial planes are more desirable to create the continuous surface.

2.3.3. LPI method

Unlike the GPI, the LPI method fits specific order polynomials using all available points within a given neighborhood. The overlapping of neighborhoods suggests that the value of the fitted polynomial at the centre of the neighborhood is estimated as the predicted value. The LPI method is sensitive to the neighborhood distance. In comparison, the LPI is capable of producing surfaces that highlight the short-range variations whereas the GPI is used to identify long-term trends in the dataset.

2.3.4. RBF method

By using the RBF method, the generated surface passes through every measured value and minimizes the total curvature of the surface. Different from the GPI and the LPI methods which are inexact interpolators, the RBF method is an exact interpolator that requires the surface to pass through given points. In contrary to the IDW method, the RBF can predict the values above the maximum and below the minimum values. It is often used to create surfaces for a large number of data points (Adhikary et al., 2017; Liao et al., 2017).

2.3.5. OK method

Compared with the above-mentioned deterministic interpolation methods, the OK method is a statistical method in which the estimates are less biased with minimum variance because predictions are accompanied by standard errors (quantification of uncertainty in predicted values). The OK method also takes into account spatial

autocorrelations and statistical relationships between measured points (Wang et al., 2014). It assumes that the unknown mean is constant and estimates the predicted value by focusing on spatial components that use sampling points within the local neighborhood. The OK is based on the following model:

$$Z(s) = \mu(s) + \varepsilon(s) \quad (2)$$

where $Z(s)$ is the variable of interest; μ is an unknown constant; $\varepsilon(s)$ is an autocorrelated error term; s indicates the location that can be identified in the form of x and y coordinates where x is longitude and y is the latitude.

2.3.6. UK method

The UK method is based on the assumption that a significant spatial trend in data values exists such as sloping surfaces or localized flat terrains. This is considered as a variation of the OK method that has no trend. The trends are too difficult to be modeled by a mathematical function due to its irregularity. Therefore, a stochastic approach can be used to characterize spatial variations. The UK method proves to be effective when there are discernible trends in the data with great background knowledge of spatial statistics.

2.4. Cross-validation

When creating a continuous surface with the point data, it is necessary to assess how well each model predicts the values at unknown locations. Thus, cross-validation can be used to evaluate and compare the performance of different interpolation techniques so as to identify the best interpolation method for creating continuous surfaces. This process involves removing each data location one at a time and predicting the associated data value. The original sample is randomly partitioned into two datasets, in which one is used to train a model and the other is used to validate the model (Wang et al., 2014, 2018). Both training and validation datasets must cross-over in consecutive rounds so that each data point can be validated against each other. The root mean square error (RMSE) is used to assess the accuracy of different interpolation methods because it is the most widely used performance metric. RMSE can be calculated using the following formula:

$$\mathrm{RMSE} = \sqrt{\frac{1}{n}\sum_{i=1}^{n}(z_i - z)^2} \quad (3)$$

where z is the predicted value; z_i is the observed value at sample point i (i = 1,2, …n); n is the number of sample points. RMSE is used as the only performance metric in this study in order to perform cross-validation in a straightforward and convenient way.

2.5. Flood inundation mapping

Flood inundation mapping provides accurate geospatial information about the extent of floods, which plays a crucial role in helping decision makers assess and manage flood risks. The flood inundation mapping can be carried out by using digital elevation models (DEM) and GIS. The Shuttle Radar Topography Mission (SRTM) DEM with a spatial resolution of approximately 30 m was used in this study. This mission was flown aboard the space shuttle Endeavour in February 2000, and collected radar data spanning over 80% of the Earth's surface between 60°N and 56°N latitudes with data points posted every 1-arc second (approximately 30 m).

In this study, the flood inundation maps were produced using the "bathtub" model for assessing coastal vulnerability to flood hazards. The "bathtub" model can be used to identify areas that may be subjected to coastal flooding caused by sea level rise. The model assumes that areas with an elevation less than a projected flood level will be flooded, which is similar to a "bathtub" (Yunus et al., 2016). Specifically, the flooded areas can be determined through simulations in a GIS environment wherein the elevation in each cell of the raster DEM is compared with the projected sea level and those cells with an elevation below the projected value of sea level are considered to be flooded.

2.6. Regression analysis

Regression analysis is useful in making predictions (Wang et al., 2016). The regression model can be used to identify if there exists a statistical relationship, if any, between given variables in a dataset. To understand potential relationships between SST, air temperature and VLM in changing sea levels, a regression model was created based on the Wilkinson notation, and the formula is given as follows:

$$\mathrm{SL} = \beta_0 + \beta_1 X_1 + \beta_2 X_2 + \beta_3 X_3 \quad (4)$$

where SL represents sea level above datum, X_1 = SST, X_2 = Air Temp, and X_3 = VLM. Eq. (4) can thus be re-written as:

$$\mathrm{SL} = \beta_0 + \beta_1(\mathrm{SST}) + \beta_2(\mathrm{AirTemp}) + \beta_3(\mathrm{VLM}) \quad (5)$$

When the SL value is obtained by using Eq. (5), the change in sea level (ΔSL) can be derived as follows:

$$\Delta\mathrm{SL} = \frac{\mathrm{SL}_{\mathrm{Present}} - \mathrm{SL}_{\mathrm{Past}}}{n} \quad (6)$$

where ΔSL represents the rate of change in sea level; $\mathrm{SL}_{\mathrm{Present}}$ represents the present SL value; $\mathrm{SL}_{\mathrm{Past}}$ represents the past SL value; n is the time period. The rates of changes in sea level at different stations can be mapped by using ArcGIS.

3. Results and discussions

3.1. Comparison of interpolation methods for spatial analysis of sea level changes

On the basis of the tide gauge data, six GIS-based interpolation techniques namely IDW, GPI, LPI, RBF, UK and OK were evaluated in this study to generate the spatial patterns of sea level changes. Fig. 2 reveals that the IDW and RBF methods nearly produce a similar map of spatial patterns in sea level rise. This can be due to the fact that they are exact interpolators. Interpolation techniques can be exact or inexact interpolators. Exact interpolators generate surfaces that pass through the control points whereas inexact interpolators predict values at locations which can differ from the known value. The raster surfaces created by exact interpolators can be similar but are different from those created by inexact interpolators. However, there is a considerable spatial difference between the surfaces generated by GPI and LPI which are inexact interpolators. The possible reason for this difference can be due to the face that LPI method is known to work well for gridded values. The GPI method uses a single mathematical function for the entire dataset and thus a change in a single value has a significant effect on the map. On the other hand, the LPI method applies mathematical functions to smaller "local" subsets of the entire dataset. Therefore, a change in any value affects the result within the specified window of data points. Also, it can be seen that the OK method has the smallest range while the LPI method has the largest range of values.

The interpolation results were also compared against each other based on the RMSE values obtained through cross-validation. As shown in Table 1, the derived RMSE values for different interpolation methods follow the following order: RBF < UK = OK < LPI < GPI < IDW. This indicates that the RBF method has the lowest RMSE and is thus the most optimal method that can be used to understand the spatial patterns of sea level rise. The geostatistical methods of UK and OK also perform well in terms of the RMSE values. A common visual pattern observed in all six methods is the low rates of sea level rise along the western coast of Australia. On the contrary, the higher rates of sea level rise patterns are observed in Bangladesh (Southern Asia). The regions with the high rates of increase in sea level were further explored in this

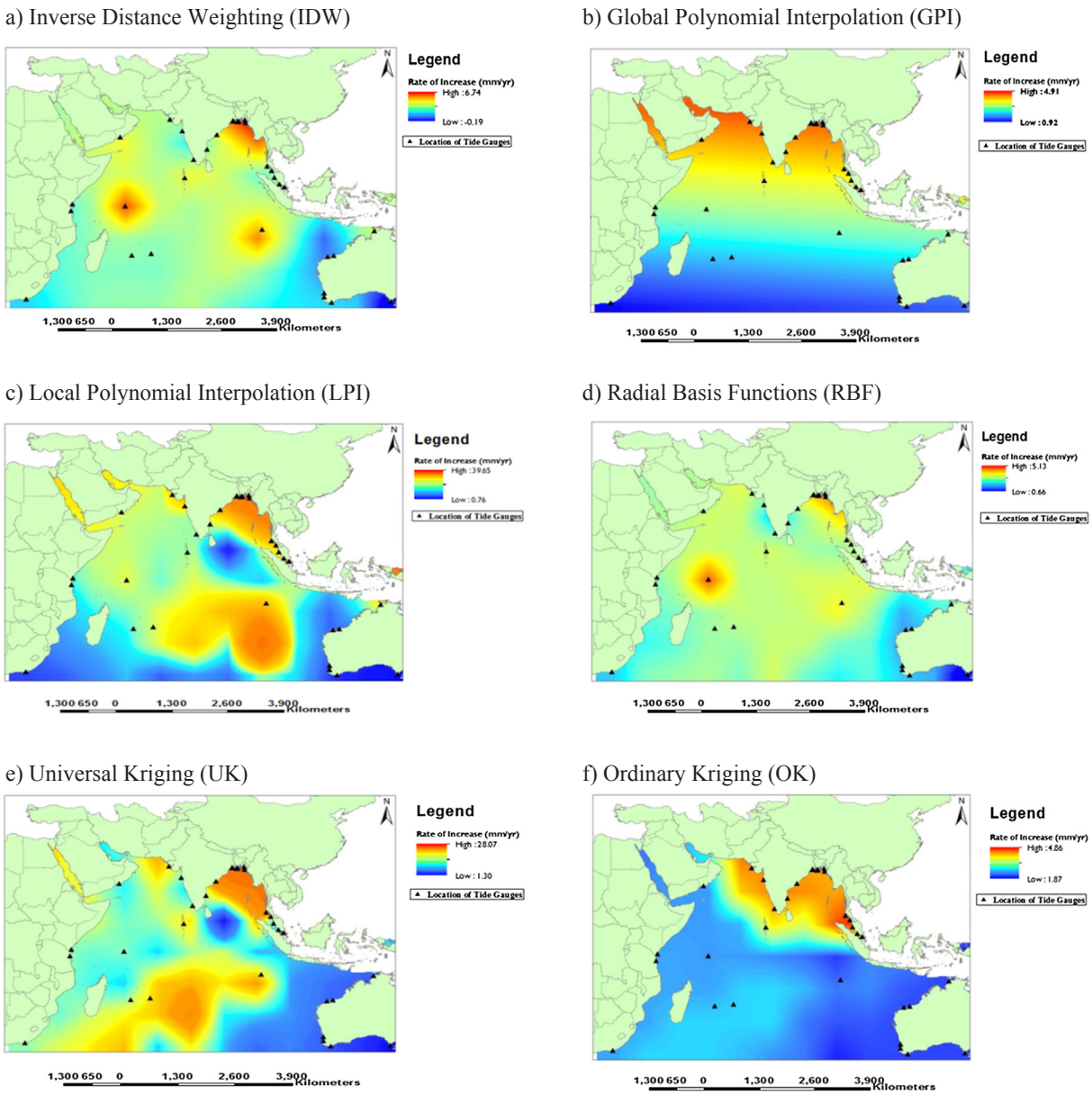

Fig. 2. Spatial patterns of sea level changes generated by using different interpolation techniques.

Table 1
Values of RMSE derived using different interpolation methods.

Interpolation method	RMSE (mm year^{-1})
IDW	3.922
GPI	3.517
LPI	3.512
RBF	3.409
UK	3.490
OK	3.490

study.

By using the RBF interpolation method, we performed spatial analysis of sea level change patterns. In Fig. 3, it can be seen that the countries lying in northeastern and central parts of the Indian Ocean are facing higher threats of sea level rise. Countries in Indonesia, Middle East and India also face a moderate risk of sea level rise. In comparison, the western coast of Australia is found to have the least rise in sea level. Thus, the regions that are facing greater increases in coastal sea level rise include Bangladesh (Southern Asia), Seychelles (Africa), and Cocos (Keeling) Islands.

3.2. Examination of potential factors affecting sea level

By using the SST, air temperature and ALT-TG values, a regression model is created to examine the importance of potential factors on sea level at the tide gauge station in Seychelles. The regression model is given as:

$$SL = 8477.6 + 39.134(SST) + 128.31(AirTemp) - 0.86(VLM) \quad (7)$$

Eq. (7) indicates that an increase in SST and air temperature can lead to an increase in sea level. As for land motions, the downward motion or subsidence of land can lead to an increase in sea level above the datum. Table 2 shows significance levels of regression coefficients for all stations. The *t*-statistic is used to examine the importance of each factor. The greater the magnitude of *t*-value that can be either positive or negative, the more important the factor. It indicates that air temperature is more important than SST and VLM for the tide gauge station in Seychelles. Similarly, for Cocos (Keeling) Islands, the regression model is created as:

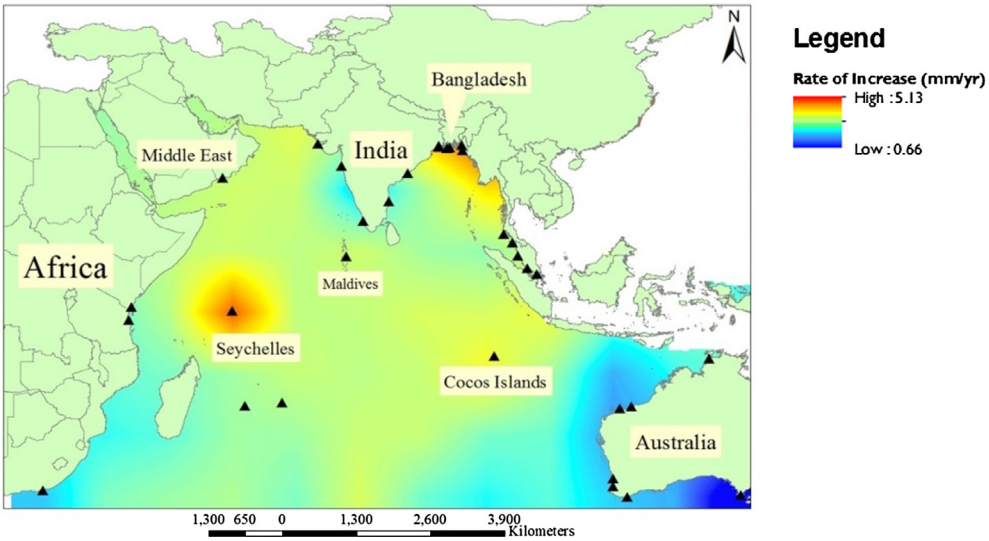

Fig. 3. Spatial pattern of sea level rise generated by using the optimal interpolation method of RBF.

Table 2
Significance levels of regression coefficients for all stations.

Regression coefficient	*t*-statistic
Seychelles	
SST	0.84
Air Temp	1.59
VLM	−1.41
Cocos (Keeling) Islands	
SST	−0.78
Air Temp	1.22
VLM	−7.34
Cox's Bazar	
SST	2.54
Air Temp	−0.16
Hiron Point	
SST	−0.30
Air Temp	0.80
Chittagong	
SST	−0.04
Air Temp	2.20
Khepupara	
SST	−1.19
Air Temp	0.40

$$SL = 22011 - 25.93\ (SST) + 37.86\ (AirTemp) - 2.174\ (VLM \quad (8)$$

Eq. (8) shows an inverse relationship between SST and sea level, indicating that an increase in SST may lead to a decrease in sea level. In addition, the VLM's contribution to sea level changes is much more significant than that for the tide gauge station in Seychelles. Due to the unavailability of ALT-TG for land movements in Bangladesh, regression models are created with only two factors including SST and air temperature at different tide gauge stations in Bangladesh. For Cox's Bazar, the regression model is created as:

$$SL = 4942.8 + 13.167\ (SST) + 65.024\ (Air\ \ Temp) \quad (9)$$

Eq. (9) indicates that both SST and air temperature have a positive impact on sea level. In other words, an increase in SST and air temperature can cause an increase in sea level at Cox's Bazar. For Hiron Point, the regression model is generated as:

$$SL = 6594.3 - 15.355\ (SST) + 34.703\ (Air\ \ Temp) \quad (10)$$

Eq. (10) indicates that an increase in air temperature or a decrease in SST can cause sea level rise. For Chittagong, the regression model is derived as:

$$SL = 3010.1 - 3.270\ (SST) + 159.42\ (Air\ \ Temp) \quad (11)$$

Eq. (11) indicates a similar relationship as compared to that for the tide gauge station at Hiron Point. Nevertheless, the importance of air temperature is much more significant at Chittagong. For Khepupara, the regression model is obtained as:

$$SL = 10279 - 157.98(SST) + 43.286(AirTemp) \quad (12)$$

Eq. (12) indicates that there is a positive relationship between air temperature and sea level. And SST has a much larger contribution to sea level changes in comparison to that of the tide gauge station at Chittagong. It should be noted that the regression models created with only SST and air temperature cannot be used to predict sea level in Bangladesh due to the poor R^2 values less than 0.5. In comparison, the regression models created with SST, air temperature and VLM for Seychelles and Cocos (Keeling) Islands have relatively larger R^2 values of 0.53 and 0.79, respectively. Results reveal that VLM has a significant impact on sea level of the Indian Ocean and thus the regression models created without VLM can result in poor performance. Future studies should be undertaken to take into account more potential factors affecting sea level when more data become available.

3.3. Temporal variations in sea level and consequent impacts on coastal flooding

Sea level rise is a big concern due to its damaging impacts on coastal regions and is considered the most significant effect on coastal flooding. Thus, the sea level trends measured by tide gauges and the consequent impacts on coastal flooding were examined in this study for the three regions of Bangladesh, Seychelles and Cocos Islands with the highest rates of sea level rise.

Bangladesh is a low-lying and densely populated riverine country, which is one of the world's most flood-prone countries. Most of the region in Bangladesh is covered by the Ganges-Brahmaputra delta and is rich in fertile flat land due to its proximity to the coast. The country has 700 rivers and 8046 km of inland waterways and is home to the Sundarbans which is the largest mangrove forest in the world. Most places have elevations of less than 10 m above the sea level while the southern coastal regions are relatively flat lands which are generally at the sea level. Climate change takes a huge toll on the country. Heavy rain falls, flooding, tidal bores and storm surges ravage the country and its coastline every year. Annual monsoon flooding results in loss of

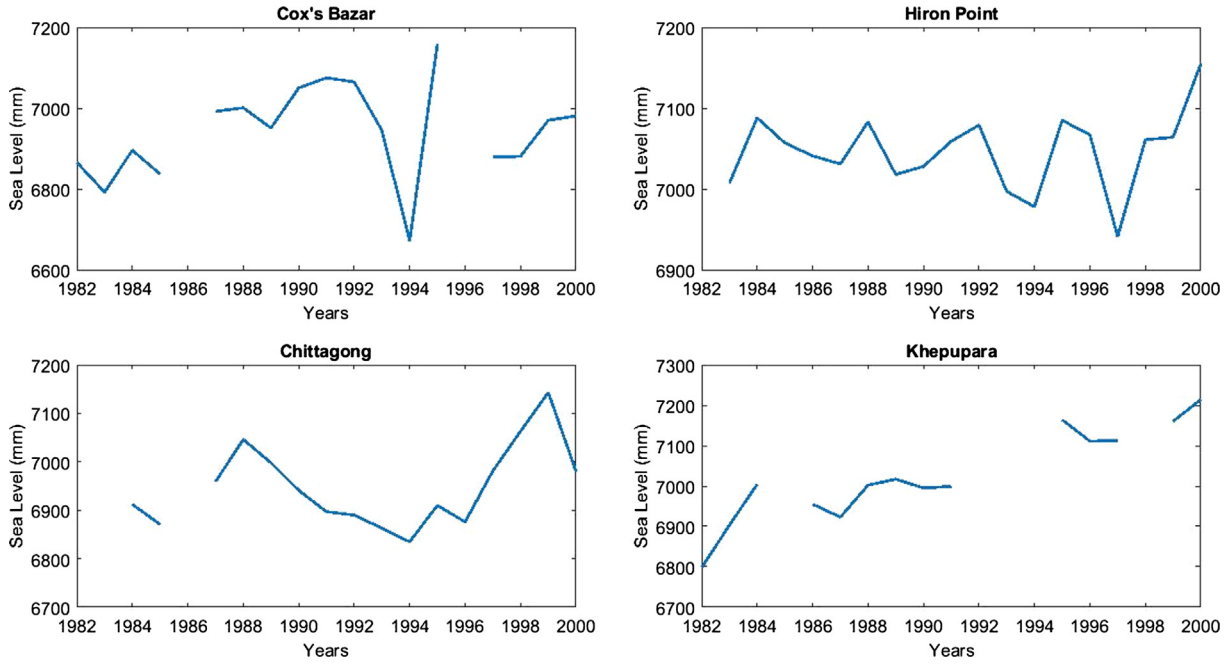

Fig. 4. Sea level trends observed at Cox's Bazar, Hiron Point, Chittagong, and Khepupara.

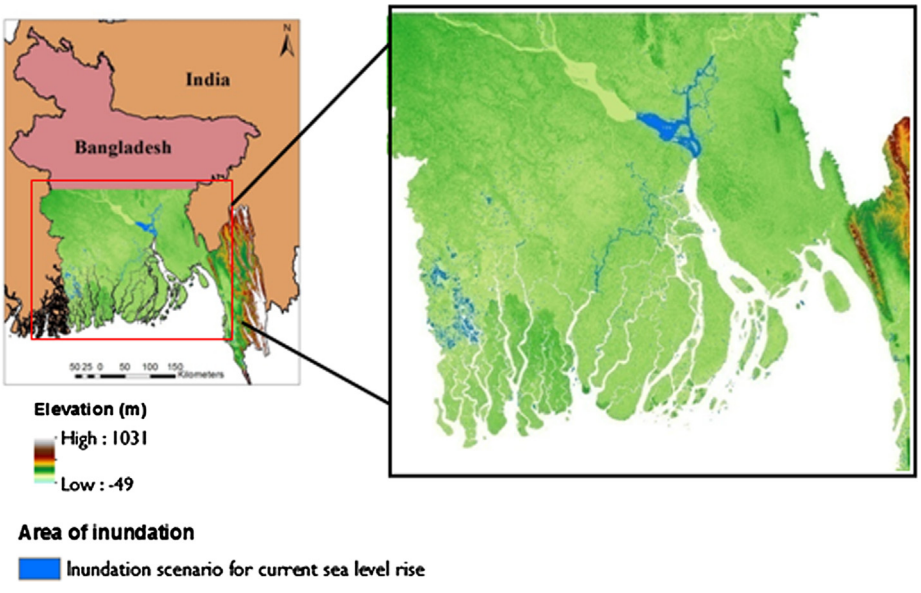

Fig. 5. Coastal flooding impact areas under current sea level scenario in Bangladesh.

human life, property damage shortage of drinking water and spread of diseases.

In this study, tide gauge data from four stations were used to identify the sea level trends in Bangladesh. Fig. 4 shows the increasing trends in sea level at four stations located along the coastlines of Bangladesh. All stations seem to have a positive sea level rise based on the historical data. At Cox's Bazar, the sea level appears to rise at the rate of 3.57 mm/year. Between the period from 1982 to 1990, there is a sharp increase in the sea level. At Hiron Point, the sea level rises by 6.1 mm/year. This increase is the slowest out of the four stations where there is a low change between the years from 1984 to 1999. At Chittagong, the rate of sea level rise is 9.47 mm/year and is characterized by highs and lows in the measurement period. Khepupara experiences a sea level rise of 17.90 mm/year which is the highest of the four stations. It can be seen that the trend continues to increase every year. The sea level rise at Khepupara and Hiron Point is due to its location on the Ganges-Brahmaputra-Meghna (GBM) river delta and therefore is prone to subsidence which is a probable factor for sea level rise.

A flood inundation map can be produced based on the fact that the average sea level rise derived from tide gauge measurements is approximately 9.2 mm/year in Bangladesh. Based on the current trend of sea level rise, the inundated area is 1531.37 km^2 which accounts for approximately 1.03% of the total land area of Bangladesh (Fig. 5). Besides the flooding from rivers, certain regions are also likely to suffer from floods under the current scenario. As shown in Fig. 6, the inundated area will be 3515.3 km^2 which accounts for approximately 2.38% of the total area of Bangladesh if the sea level rises by 1 m. For the western region of Bangladesh, a rise of 1 m in sea level can cause flooding problems for the coastline in the west. In addition, the deltaic regions are also prone to flooding as indicated by "blue areas". There is no big difference in the flooding areas generated under current and future scenarios because a majority of coastal areas in Bangladesh is

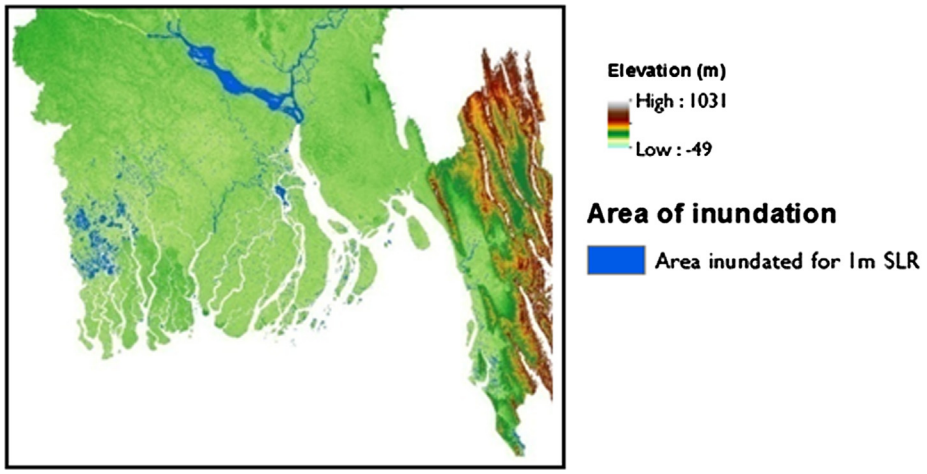

Fig. 6. Coastal flooding impact areas under the scenario of 1-m rise in sea level in Bangladesh.

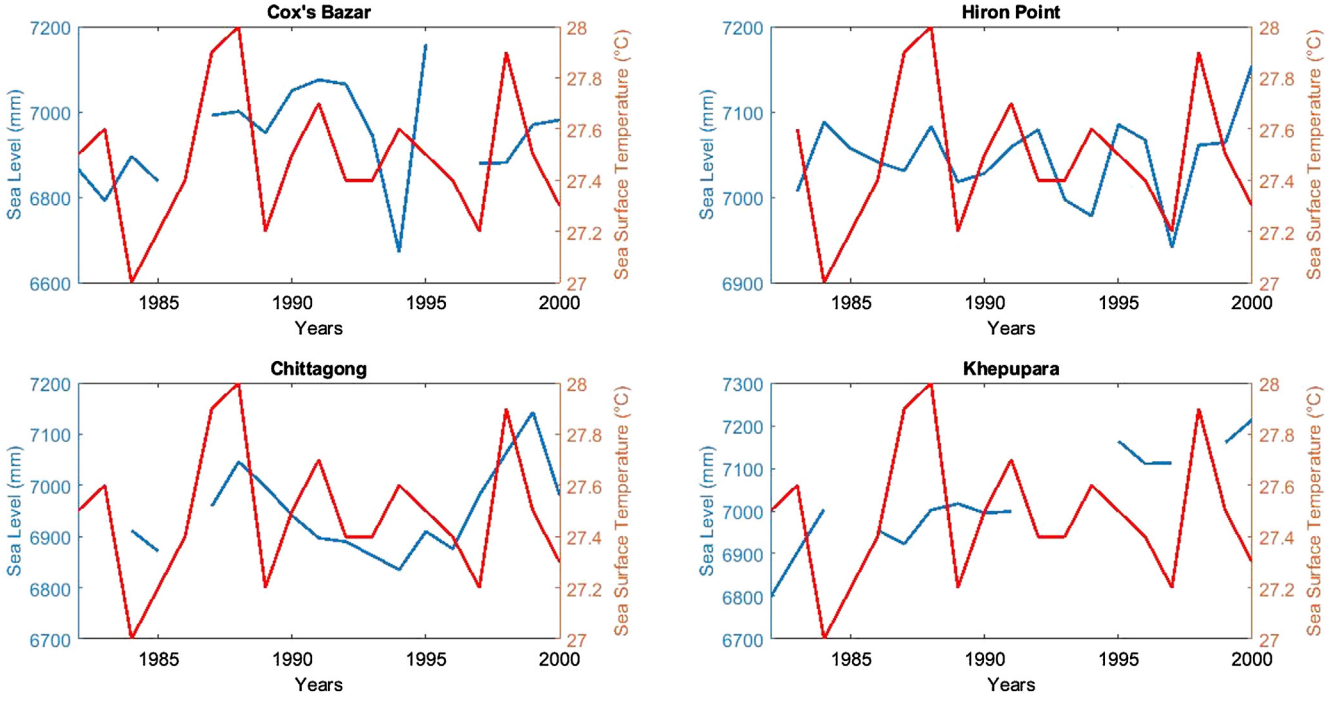

Fig. 7. Comparison of temporal changes in sea level and sea surface temperature at Cox's Bazar, Hiron Point, Chittagong, and Khepupara.

within 1–2 m above sea level. It should be noted that these maps show the inundation areas impacted only by "static" floods (i.e. floods are caused by sea level rises and not resulting from a storm surge or other combined effects). In reality, the actual flood zones are likely to be very different due to interactive effects.

Figs. 7 and 8 compare the temporal changes in sea level with sea surface temperature and air temperature at four tide gauge stations in Seychelles. Seychelles is a sovereign Africa state in the Indian Ocean off the west coast of Africa, which contains about 115 islands with a total area of 459 km^2. This country has a population of 87,000 of which 90% live on Mahé. The climate is mostly humid and is classified as tropical rainforest by the Köppen-Geiger system. There is a small variation in temperature throughout the year. Temperature on Mahé varies from 24 to 30 °C with average rainfall of 3300 mm. Fig. 9 shows that Mahé experiences a sea level rise at the rate of 5.19 mm/year.

For the inundation mapping of Seychelles, Mahé is the primary concern because it is the main island with a larger population and land area. As shown in Fig. 10, the inundated area is 3.463 km^2 which accounts for about 0.68% of the total land area. It can be seen that the northeastern and eastern coasts of Mahé are prone to flooding. If the sea level rises by 1 m, the inundated area will be 7.28 km^2 which accounts for approximately 1.5% of the total area of Seychelles (Fig. 11). Figs. 12 and 13 compare the temporal changes in sea level with SST and air temperature. Fig. 14 shows the VLM observed at Mahé by using the ALT-TG data. It reveals that the land underwent uplift and subsidence during the period from 1990 to 2012 with notable subsidence between 1999 and 2006. And the region is undergoing subsidence at the rate of 1.55 ± 0.21 mm/year.

The Cocos (Keeling) Islands are a group of low-lying atolls with an area of 14.2 km^2 in the Indian Ocean off the coast of Perth, Australia. The Australia territory harbors a coastline of 26 km and is covered with coconut palms and other vegetation. The population is estimated to be about 600. Pleasant climate prevails and is moderated by the southeast trade winds for nine months of the year with moderate rainfall. Tropical cyclones are known to occur during the early months of the year. Owing to its position midway between the Equator and the Tropic of Capricorn, the climate is characterized as tropical monsoon type by the Köppen classification system.

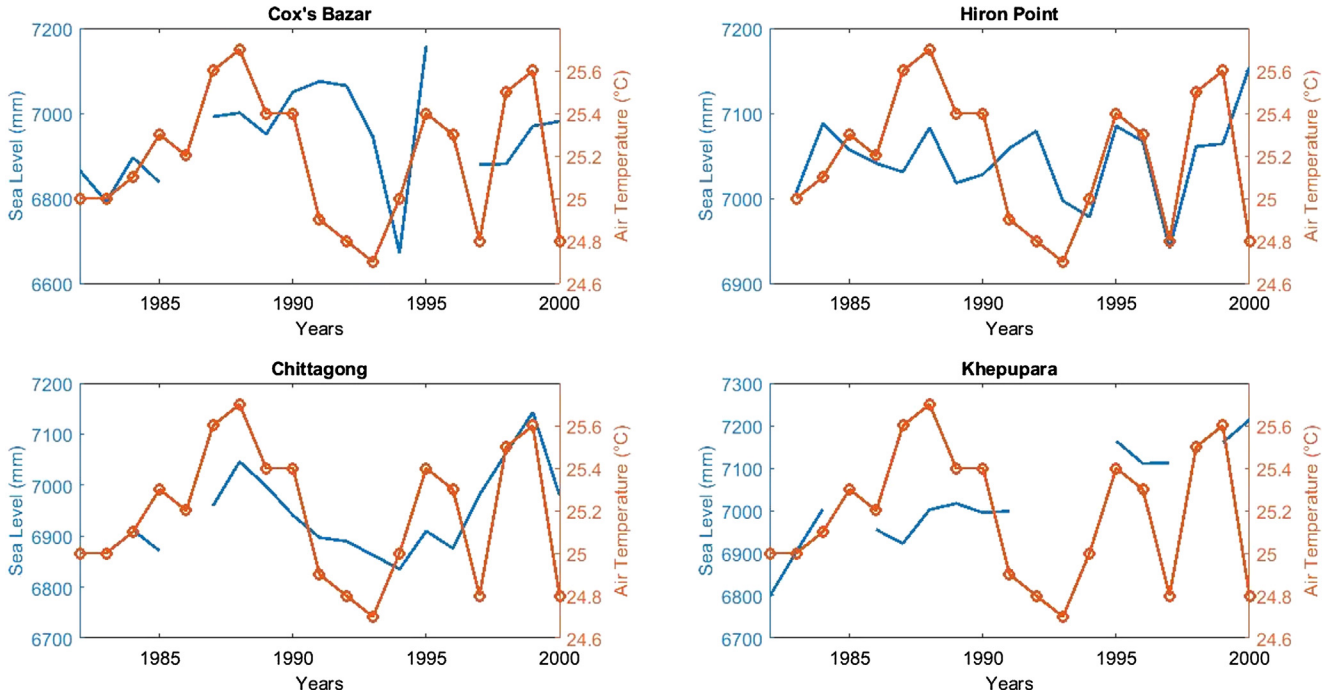

Fig. 8. Comparison of temporal changes in sea level and air temperature at Cox's Bazar, Hiron Point, Chittagong, and Khepupara.

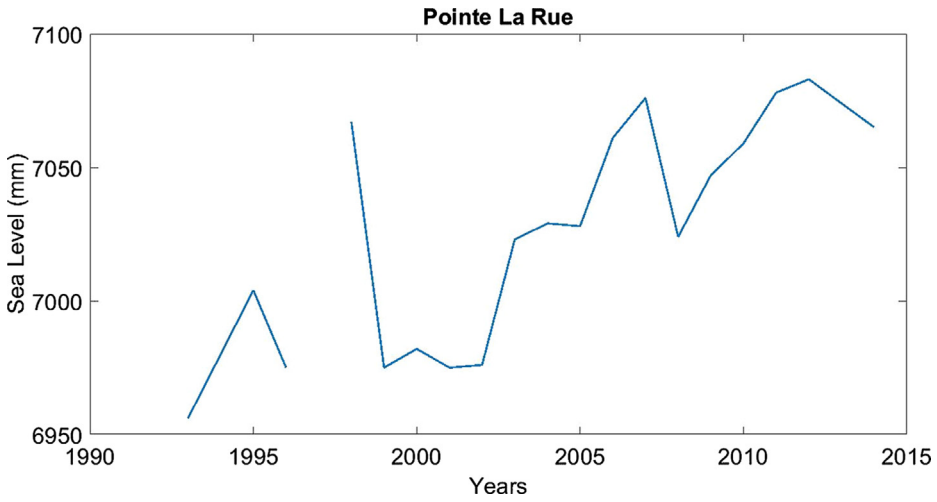

Fig. 9. Sea level trends observed at Mahé, Seychelles.

In Fig. 15, the rate of rise in sea level is 5.347 mm/year. Based on the current trend of sea level rise at Cocos Islands by using tide gauge data, the inundated area is 1.288 km^2 which accounts for about 9.14% of the land area. In Fig. 16, it can be seen that the entire coastline is at risk of flooding. And an area in the southern part of the island can be greatly affected by the current sea level trend. In Fig. 17, the inundated area will be 1.63 km^2 which accounts for approximately 11.6% of the total area of Cocos Islands if the sea level rises by 1 m in the future. Certain parts of the island in the west are prone to flooding under the scenario of 1-m rise in sea level. Figs. 18 and 19 compare the temporal changes in sea level with SST and air temperature. Fig. 20 shows the VLM observed at Cocos (Keeling) Islands. From 1993 to 2015, the land underwent subsidence with relatively high subsidence occurring during the period from 1999 to 2004. The land is undergoing subsidence at the rate of 3.89 ± 0.14 mm/year.

It should be noted that the sea level of the Indian Ocean has been rising more rapidly in recent years. For instance, the sea level for Seychelles is expected to experience a rise at the rate of 2.21 mm/year according to the sea level data collected for the period 1993–2007 (IPCC, 2007; Gerlach, 2008). In fact, the sea level for the island of Seychelles has been experiencing a rise of 5.19 mm/year based on the tide gauge data collected in recent years. Similarly, the Cocos (Keeling) Islands is expected to experience a rise in sea level at the rate of 1.5 mm/year according to the reconstructed sea level dataset collected for the period 1950–2001 (Church et al., 2006; IPCC, 2007, 2013). In fact, Cocos (Keeling) Islands has been experiencing a rise in sea level at the rate of 5.34 mm/year in recent years. These reveal that the rate of sea level rise has been increasing over time, posing a significant threat to the Indian Ocean coastal areas. According to a government report by Maunsell Australia (2009), the sea level of the Indian Ocean has risen by 9.8 mm/year by the beginning of the 21st century. Consequently, the scenario of 1-m rise in sea level was used in this study to examine potential impacts of sea level rise on coastal flooding in the Indian Ocean.

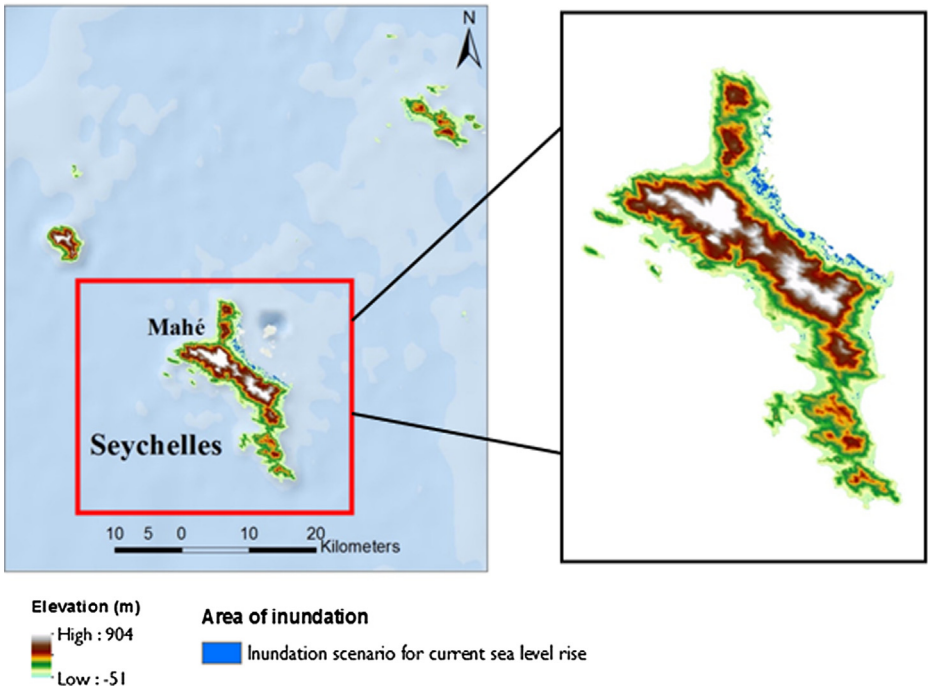

Fig. 10. Coastal flooding impact areas under current sea level scenario in Seychelles.

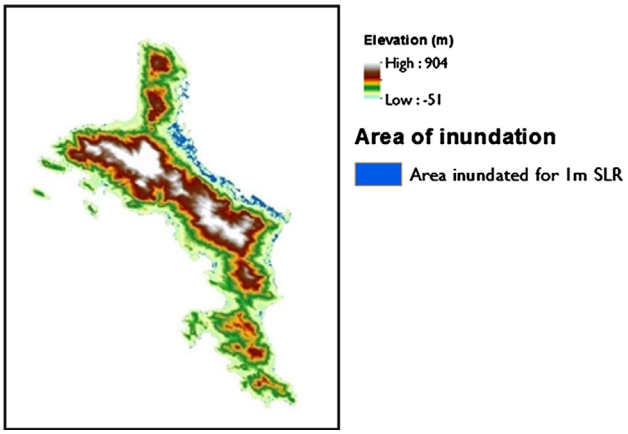

Fig. 11. Coastal flooding impact areas under the scenario of 1-m rise in sea level at Mahé, Seychelles.

4. Conclusions

In this study, we examine regional changes in sea level of the Indian Ocean and the consequent impacts on coastal flooding in a changing climate. Various interpolation methods are evaluated and compared to generate spatial patterns of sea level changes through cross-validation. The RBF interpolation method is identified as the optimal one with the smallest RMSE value, which is thus used to perform spatial analysis of sea level changes in the Indian Ocean. The regions with relatively high sea level rise and their impacts on coastal flooding are further investigated through multivariate regression analysis and inundation mapping.

Our findings reveal that VLM has a considerable impact on sea level rise and a subsidence of land can lead to an increase in the rates of sea level rise. Specifically, the inundated area is 1531.37 km^2 that accounts for approximately 1.03% of the total land area of Bangladesh based on the current trend of sea level rise. And the inundated area will become 3515.3 km^2 that accounts for approximately 2.38% of the total land area if the sea level rises by 1 m in the future. Due to the unavailability

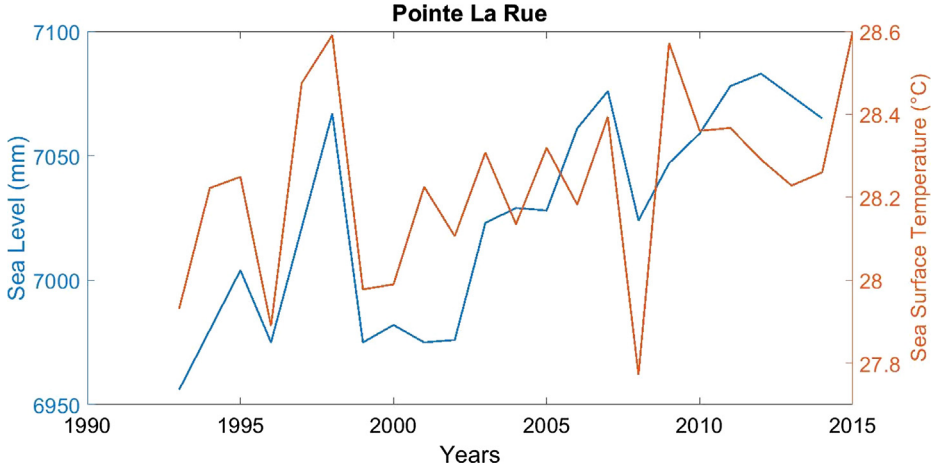

Fig. 12. Comparison of temporal changes in sea level and sea surface temperature in Seychelles.

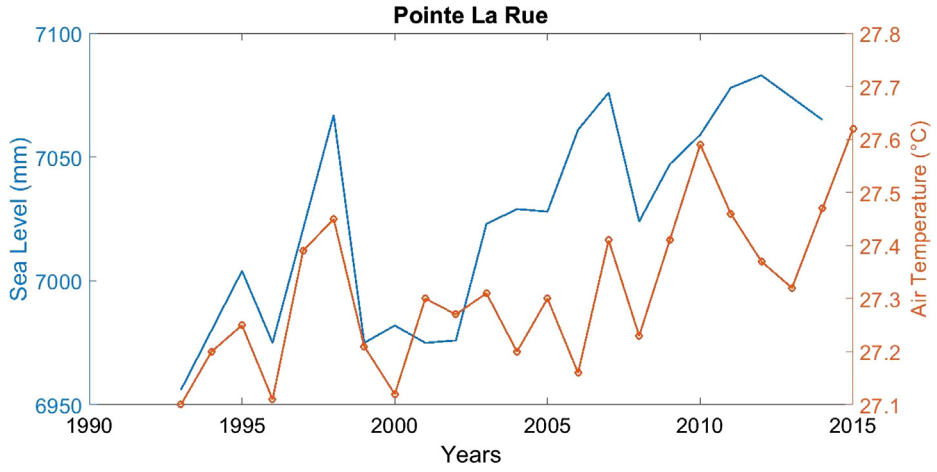

Fig. 13. Comparison of temporal changes in sea level and air temperature in Seychelles.

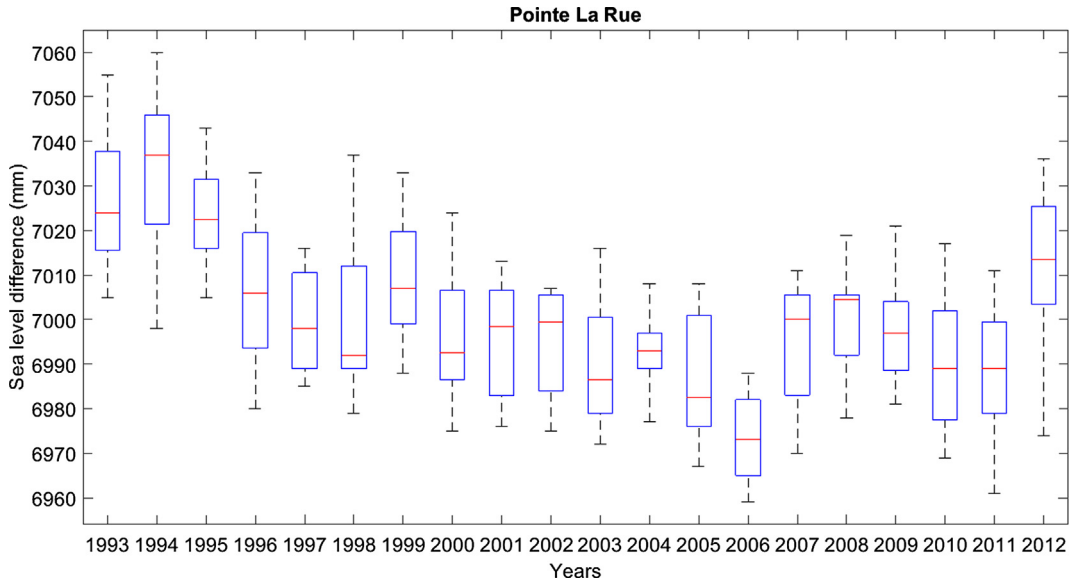

Fig. 14. Difference in sea levels (vertical land motions) observed by altimetry measurements at Mahé, Seychelles.

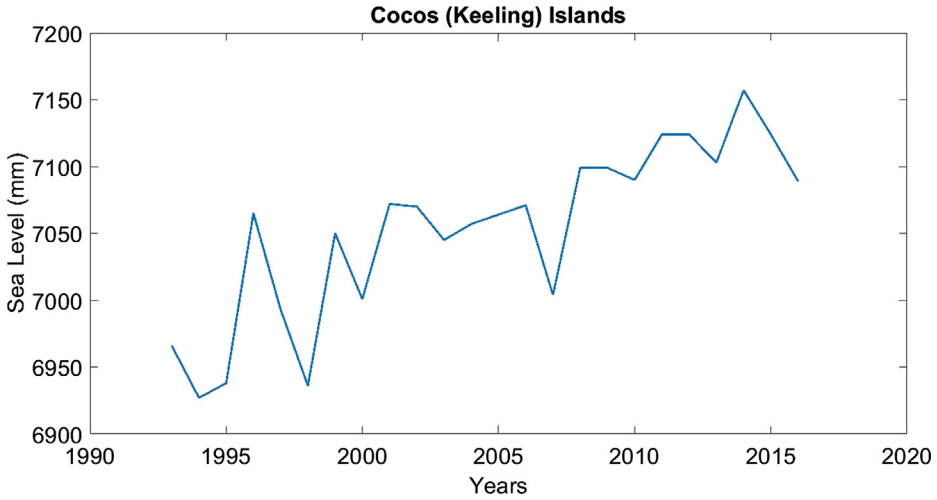

Fig. 15. Sea level trends observed at Cocos (Keeling) Islands.

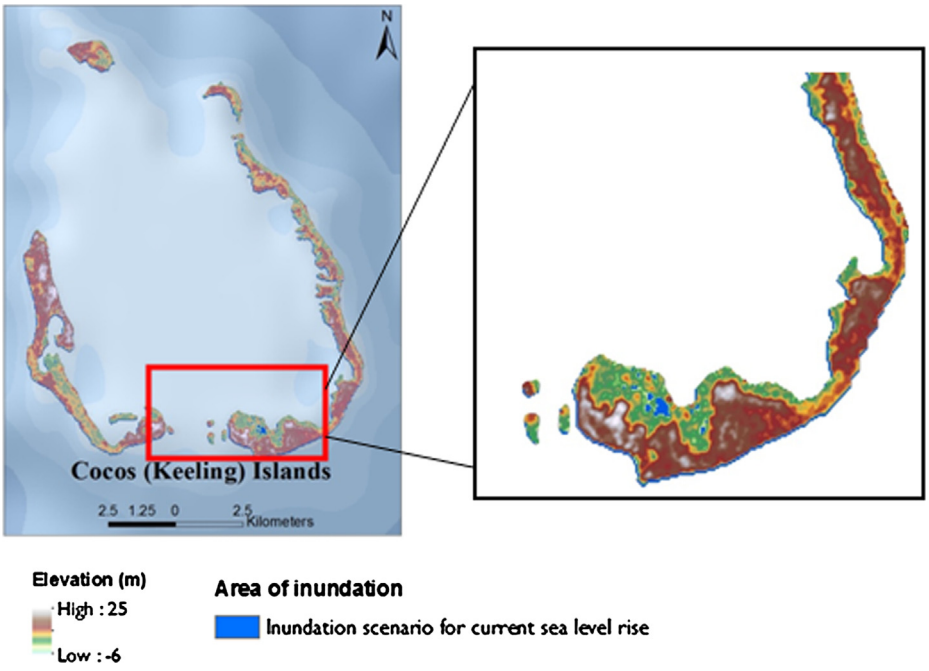

Fig. 16. Coastal flooding impact areas under current sea level scenario at Cocos (Keeling) Islands.

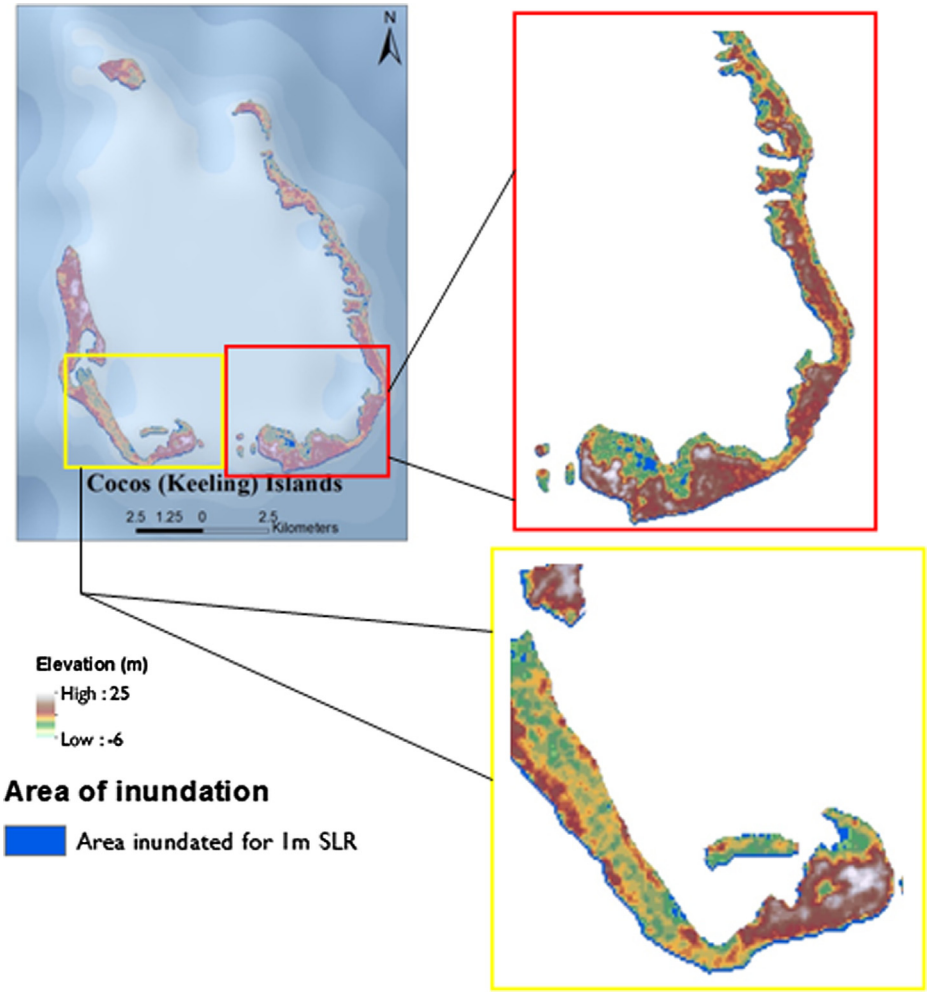

Fig. 17. Coastal flooding impact areas under the scenario of 1 m rise in sea level at Cocos (Keeling) Islands.

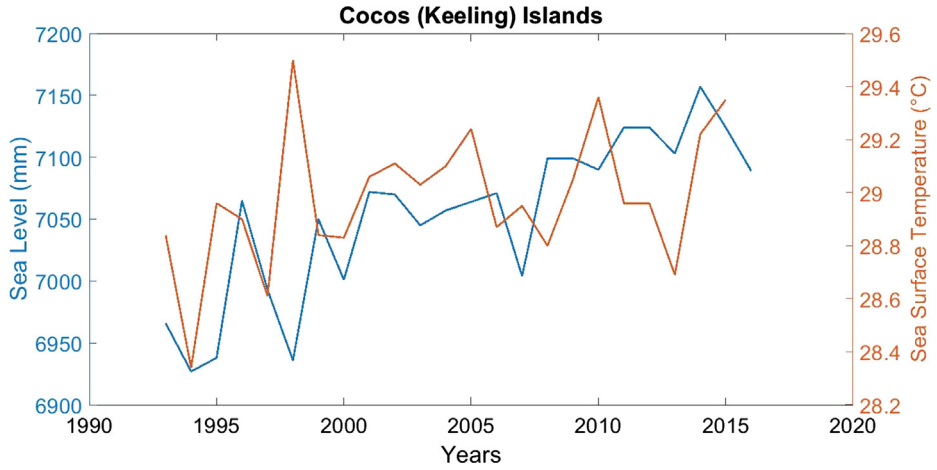

Fig. 18. Comparison of temporal changes in sea level and sea surface temperature at Cocos (Keeling) Islands.

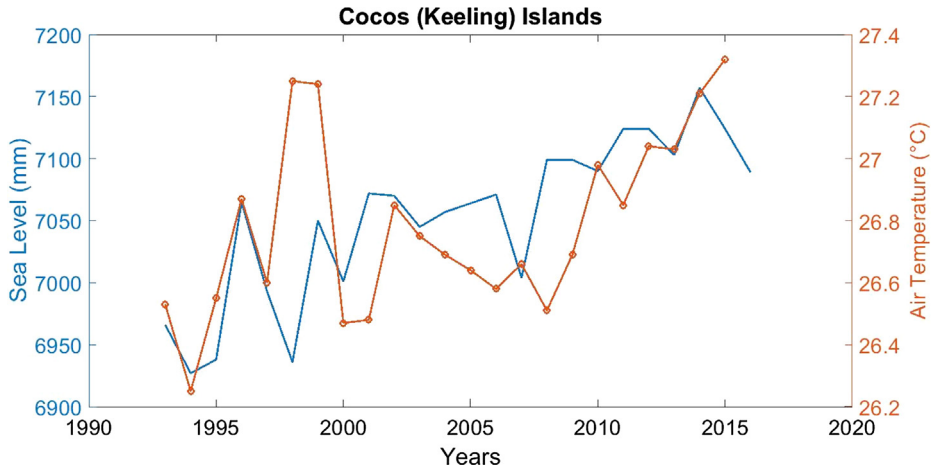

Fig. 19. Comparison of temporal changes in sea level and air temperature at Cocos (Keeling) Islands.

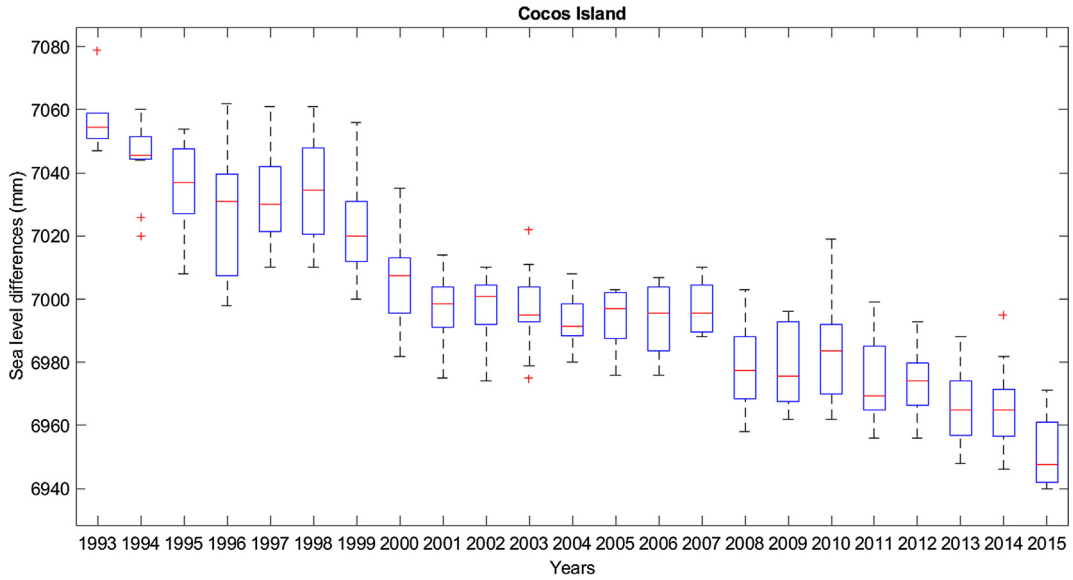

Fig. 20. Difference in sea levels (vertical land motions) observed by altimetry measurements at Cocos (Keeling) Islands.

of the VLM data for Bangladesh, it is impossible to deduce its relationship with sea level changes. For the region of Seychelles, the inundated area is 3.463 km^2 that accounts for about 0.68% of the total land area under the current scenario. And the northeastern and eastern coasts of Mahé are prone to flooding. If the sea level rises by 1 m, the inundated area will become 7.28 km^2 that accounts for approximately 1.5% of the total area of Seychelles. In addition, land subsidence has a considerable impact on sea level rise in Seychelles. And the region is

undergoing subsidence at the rate of 1.55 ± 0.21 mm/year. At Cocos Islands, the inundated area is 1.288 km^2 that accounts for about 9.14% of the land area under the current scenario. The inundated area will become 1.63 km^2 that accounts for approximately 11.6% of the total area of Cocos Islands if the sea level rises by 1 m in the future. And certain parts of the island in the west are prone to flooding under the future scenario. Moreover, the land is undergoing subsidence at the rate of 3.89 ± 0.14 mm/year at Cocos Islands.

This study is a first attempt to examine regional changes in sea level of the Indian Ocean and potential coastal flooding impacts by using tide gauge data. The methods used in this study can be applied to other coastal regions around the world. Since the flood inundation maps were produced in this study based on standard "bathtub" model which did not take into account the dynamic nature of coastal flooding, future studies will be undertaken to perform dynamic coastal flooding simulations in order to improve the accuracy of flood impact assessment. Moreover, linear regression was used to examine potential factors affecting sea level. Such an assumption of linearity oversimplifies the complex relationships between sea level changes and influencing factors, which may result in poor performance. It is thus necessary to develop nonlinear regression models with more potential factors affecting sea level in order to improve model performance. Since only tide gauge data was used in this study, any interpolation of the non-coastal zones (i.e. in the middle of the ocean) cannot be validated due to the sparse data. Other types of data such as satellite imagery and LiDAR data should also be used in future studies to enhance the reliability of spatial analysis of sea level changes. In addition, it is necessary to examine the impact of the spatial resolution of DEM on flood inundation mapping in order to improve the accuracy of coastal flood risk assessment.

Acknowledgments

This research was supported by the National Natural Science Foundation of China (Grant No. 51809223) and the Hong Kong Polytechnic University Start-up Grant (Grant No. 1-ZE8S). The authors would like to express their sincere gratitude to the editor and anonymous reviewers for their constructive comments and suggestions.

References

Adhikary, S.K., Muttil, N., Yilmaz, A.G., 2017. Cokriging for enhanced spatial interpolation of rainfall in two Australian catchments. Hydrol. Process. 31, 2143–2161.
Agnew, M., Palutikof, J., 2000. GIS-based construction of baseline climatologies for the Mediterranean using terrain variables. Clim. Res. 14, 115–127.
Baki, H., Shum, C.K., 2000. Mean sea level variation in the South China Sea from four decades of tidal records in Hong Kong. Mar. Geod. 23, 221–233.
Church, J.A., White, N.J., Coleman, R., Lambeck, K., Mitrovica, J.X., 2004. Estimates of the regional distribution of sea-level rise over the 1950 to 2000 period. J. Clim. 17, 2609–2625.
Church, J.A., White, N.J., Hunter, J.R., 2006. Sea level rise at tropical Pacific and Indian Ocean islands. Global Planet. Change 53, 155–168.
Chepurin, G.A., Carton, J., 2013. Sea level in ocean reanalyses and tide gauges. J. Geophys. Res. Oceans 119, 147–155.
Fenoglio, L., Becker, M., Manurung, P., 2012. Sea level change and vertical motion from satellite altimetry, tide gauges and GPS in the Indonesian region. Mar. Geod. 35, 137–150.
Gerlach, J., 2008. Climate change and identification of terrestrial protected areas in the Seychelles Islands. Biodiversity 9, 24–29.
Gornitz, V., 2013. Rising Seas – Past, Present, Future. Columbia University Press, New York, NY.
Han, W., et al., 2010. Patterns of Indian Ocean sea level change in a warming climate. Nat. Geosci. 3, 546–550.
Hay, C.C., Morrow, E., Kopp, R.E., Mitrovica, J.X., 2015. Probabilistic reanalysis of twentieth-century sea-level rise. Nature 517, 481–484.
IPCC (Intergovernmental Panel on Climate Change), 2007. Climate Change 2007: The Physical Science Basis. Contribution of Working Group I to the Fourth Assessment Report of the IPCC. Cambridge: Cambridge University Press.
IPCC (Intergovernmental Panel on Climate Change), 2013. Climate Change 2013: The Physical Science Basis. Contribution of Working Group I to the Fifth Assessment Report of the IPCC. Cambridge: Cambridge University Press.
Keskin, M., Dogru, A.O., Balcik, F.B., Goksel, C., Ulugtekin, N., Sozen, S., 2015. Comparing spatial interpolation methods for mapping meteorological data in Turkey. Energ. Syst. Manage. 33–42.
Li, Y., Han, W., 2015. Decadal sea level variations in the Indian Ocean investigated with HYCOM: roles of climate modes, ocean internal variability, and stochastic wind forcing. J. Clim. 28, 9143–9165.
Liao, Z., Dong, Q., Xue, C., Bi, J., Wan, G., 2017. Reconstruction of daily sea surface temperature based on radial basis function networks. Remote Sens. 9, 1204.
Maunsell Australia, 2009. Climate Change Risk Assessment for the Australian Indian Ocean Territories. Commonwealth Attorney-General's Department. Canberra: Australia.
Merrifield, M.A., Leuliette, E., Thompson, P., Chambers, D., Hamlington, B.D., Jevrejeva, S., Marra, J.J., Menéndez, M., Mitchum, G.T., Nerem, R.S., Sweet, W., 2016. Sea level variability and change. Bull. Amer. Meteor. Soc. 97, S80–S82.
Míguez, B., Testut, L., Wöppelmann, G., 2012. Performance of modern tide gauges: towards mm-level accuracy. Adv. Span. Phys. Oceanogr. 221–228.
Pramanik, M.K., Biswas, S.S., Mukherjee, T., Roy, A.K., Pal, R., Mondal, B., 2015. Sea level rise and coastal vulnerability along the eastern coast of India through geospatial technologies. J. Remote Sens. GIS 4, 2469–4134.
Qin, X.S., Lu, Y., 2014. Study of climate change impact on flood frequencies: a combined weather generator and hydrological modeling approach. J. Hydrometeorol. 15, 1205–1219.
Roxy, M., Ritika, K., Terray, P., Masson, S., 2014. The curious case of Indian Ocean warming. J. Clim. 27, 8501–8509.
Sweet, W.V., Kopp, R.E., Weaver, C.P., Obeysekera, J., Horton, R.M., Thieler, E.R., Zervas, C., 2017. Global and Regional Sea Level Rise Scenarios for the United States. NOAA Technical Report NOS CO-OPS 083.
Khan, T.M.A., Singh, O.P., Rahman, M.S., 2000. Recent sea level and sea surface temperature trends along the Bangladesh coast in relation to the frequency of intense cyclones. Mar. Geod. 23, 103–116.
Thompson, P.R., Piecuch, C.G., Merrifield, M.A., McCreary, J.P., Firing, E., 2016. Forcing of recent decadal variability in the Equatorial and North Indian Ocean. J. Geophys. Res. Oceans 121, 6762–6778.
Wang, S., Ancell, B.C., Huang, G.H., Baetz, B.W., 2018. Improving robustness of hydrologic ensemble predictions through probabilistic pre- and post-processing in sequential data assimilation. Water Resour. Res. 54, 2129–2151.
Wang, S., Huang, G.H., Baetz, B.W., Huang, W., 2016. Probabilistic inference coupled with possibilistic reasoning for robust estimation of hydrologic parameters and piecewise characterization of interactive uncertainties. J. Hydrometeorol. 17, 1243–1260.
Wang, S., Huang, G.H., Baetz, B.W., Huang, W., 2015. A polynomial chaos ensemble hydrologic prediction system for efficient parameter inference and robust uncertainty assessment. J. Hydrol. 530, 716–733.
Wang, S., Huang, G.H., Lin, Q.G., Li, Z., Zhang, H., Fan, Y.R., 2014. Comparison of interpolation methods for estimating spatial distribution of precipitation in Ontario, Canada. Int. J. Climatol. 34, 3745–3751.
Wöppelmann, G., Marcos, M., 2016. Vertical land motion as a key to understanding sea level change and variability. Rev. Geophys. 54, 64–92.
Yunus, A.P., Avtar, R., Kraines, S., Yamamuro, M., Lindberg, F., 2016. Uncertainties in tidally adjusted estimates of sea level rise flooding (bathtub model) for the Greater London. Remote Sens. 8, 366.